



Glycosyl Thiourea: Synthesis, Cyclization, Reaction, Molecular Docking, and Evaluation as Potential Acetylcholinesterase Inhibitors



Salma A. Ellithy*¹; Adel A-H Abdel-Rahman¹; Nasser A. Hassan*^{2,3}; Mohamed Elsawalhy¹; Eman S. Abou-Amra⁴; Allam, A. Hassan⁵

¹ Department of Chemistry, Faculty of Science, Menoufia University, Shibin El-Kom 32511, Egypt

² Department of Photochemistry (Synthetic Unit), National Research Centre, 12622 Cairo, Egypt

³ Department of Pharmaceutical Sciences, College of Pharmacy, Shaqra University, Shaqra 11961, Saudi Arabia

⁴ Department of Chemistry, Faculty of Science (Girls), Al-Azhar University, Nasr City, Cairo, Egypt

⁵ Department of Chemistry, Faculty of Science, Suez University, Suez 43221, Egypt

Abstract

In this research, we successfully synthesized a distinctive group of iminothiazolidinone derivatives, using glucose isothiocyanate as the starting material. The structural elucidation of these newly created compounds was achieved through a combination of analytical techniques, including IR, ¹H NMR, and ¹³C NMR. We then evaluated the inhibitory activity of these compounds against acetylcholinesterase (AChE) using the Ellman's method spectrophotometer, comparing their performance to standard drugs like donepezil, rivastigmine, and tacrine. Impressively, the majority of the tested compounds demonstrated inhibitory activity against AChE, with iminothiazolidinone derivative (**5a**) standing out as the most potent (IC₅₀ = 0.209 μg/mL). It even surpassed the effectiveness of rivastigmine and tacrine, coming close to the potency of donepezil. Further investigation into the potential of these compounds as AChE inhibitors for Alzheimer's disease drug development involved docking simulations using Molecular Operating Environment (MOE). Derivatives 3,5-disubstituted-(2,3,4,6-tetra-O-acetyl-β-D-glucopyranosyl) imino) thiazolidin-4-ones (**5a**), (**5f**), (**6c**) and 3,5-disubstituted-(β-D-glucopyranosyl)imino)thiazolidin-4-one (**6d**) displayed promising docking scores in MOE simulations. In *Silico* ADMET experiments assessed their pharmacokinetic and toxicity studies, demonstrating strong binding affinity and favorable interactions with the target protein. Pharmacophore models confirmed their potential as selective enzyme inhibitors through 3D virtual screening.

Keywords: Thiazolidin-4-one; 2,3,4,6-tetra-O-acetyl-β-D-glucopyranosyl isothiocyanate; pharmacokinetics prediction; Alzheimer's disease; Acetylcholine esterase

1. Introduction

Alzheimer's disease (AD) is a persistent neurodegenerative condition characterized by gradual nerve cell deterioration and a rapid decline in memory and cognitive functions—the primary cause of dementia, with its prevalence steadily rising [1].

By 2050, projections suggest that approximately one in every 85 individuals will have AD, surpassing the public health impact of AIDS, cancer, and cardiovascular diseases combined [2-4]. This underscores the urgent need for pharmaceutical

researchers to discover effective treatments for Alzheimer's disease [5,6].

While the exact causes of AD remain incompletely understood, it is widely recognized as a complex condition influenced by numerous neurochemical factors [7]. Several potential molecular pathways, including the β-amyloid cascade [8], cholinergic dysfunction [9], and various other well-documented mechanisms and hypotheses [10-16], have been suggested. These findings not only inspire the development of new AD treatments but also shed

*Corresponding author e-mail: salma_yousf_26@yahoo.com, nasserabdelhamid@hotmail.com

EJCHEM use only: Received date 24 October 2023; revised date 29 November 2023; accepted date 30 November 2023

DOI: 10.21608/EJCHEM.2023.244506.8770

©2023 National Information and Documentation Center (NIDOC)

light on the intricate nature of the disease. Current AD treatment primarily relies on cholinesterase inhibitors, such as donepezil, galantamine, tacrine, rivastigmine, Huperzine A, memantine, and the recently approved monoclonal antibody Aducanumab. Aducanumab specifically targets β A aggregates [Fig. 1] [17]. While these treatments have demonstrated effectiveness in enhancing cholinergic neurotransmission and reducing β A protein deposits, they are associated with various side effects and provide only moderate relief from symptoms, doing little to slow down the disease [18]. Researchers are actively seeking novel treatments targeting specific disease mechanisms to interfere with AD progression, particularly focusing on "one molecule multi-targeting" compounds recognized as hybrid therapeutic molecules. These compounds consist of two or more bioactive moieties with complementary pharmacological properties, facilitating a synergistic effect [19].

Heterocyclic compounds containing nitrogen and sulfur atoms have gained significant interest in synthetic organic and medicinal chemistry [20,21]. Thiazole derivatives, a versatile scaffold for developing various bioactive molecules, has shown promise with a wide range of pharmacological properties, including anti-HIV, anti-tumor, anti-inflammatory, antimicrobial, and enzyme inhibition such as acetyl/butyrylcholinesterase [Fig. 2] [22-27]. Sugar isothiocyanates, pivotal in carbohydrate chemistry, facilitate the formation of diverse functional groups and their attachment to saccharides. Their versatility extends to organic chemistry, biochemistry, and pharmaceutical research, with potential benefits in drug development. Moreover, their application in the flavor and fragrance industry, along with potential use in sustainable agriculture, awaits further research on properties and regulatory approval [17,21-26].

Glycosides have also shown potential as protective candidates for AD treatment [28]. In our ongoing efforts to develop efficient methods for synthesizing medicinal heterocycles [29-35], we conducted a straightforward chemical reaction to create novel iminothiazolidinone derivatives using glucose isothiocyanate. These compounds, which share structural similarities with donepezil and acetylcholinesterase (AChE), could potentially act as AChE inhibitors, offering new possibilities for

Alzheimer's disease (AD) treatment

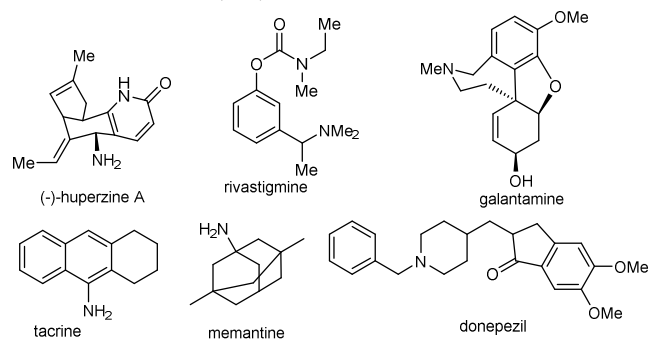


Figure 1: FDA-Approved Cholinesterase Inhibitors for AD

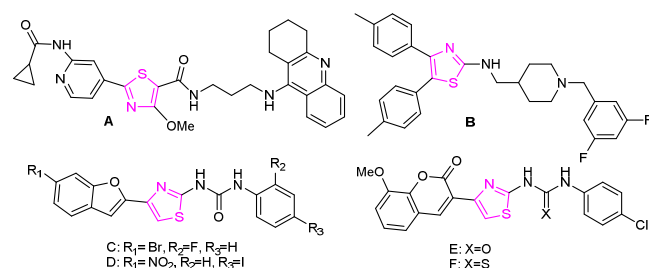


Figure 2: Reported Thiazole-Based AChE Inhibitors (A-F)

2. Materials and methods

2.1 Experimental section

2.1.1 Synthesis methods

All melting points are uncorrected and were measured using an Electro thermal IA 9100 apparatus. The ^1H NMR and ^{13}C NMR spectra were measured on a BRUKER 400 MHz for ^1H NMR and 100 MHz for ^{13}C NMR at Faculty of Science, Zagazig University and Cairo University, Egypt. The coupling constants (J) were given in Hertz. The chemical shifts are expressed on the δ (ppm) scale using TMS as the standard reference. The FT-IR spectra were recorded on a Shimadzu IR 8400s spectrophotometer (KBr, $\nu_{\text{max}}/\text{cm}^{-1}$) at the Micro Analytical Laboratory, Cairo University, Egypt. The microanalytical data were carried out on a Vario El-Mentar instrument, at the Micro Analytical Laboratory, National Research Center, Cairo, Egypt. The reactions were monitored by thin layer chromatography (TLC). TLC was performed on Macherey-Nagel aluminum-backed plates, pre-coated with silica gel 60 (UV254). Column chromatography was carried out on silica gel 60 (0.040–0.063 mm)

under flash conditions. All chemicals and solvents were purchased from Sigma-Aldrich, Alfa Aesar and ACROS Organics and used as provided. 2,3,4,6-tetra-O-acetyl- β -D-glucopyranosyl isothiocyanate [36,37] was prepared by the reaction of per-O-acetylated- β -D-glucopyranosyl bromide with lead thiocyanate in dry toluene [38] according to the literature procedure.

1-(4-Fluorobenzyl)-3-(2,3,4,6-tetra-O-acetyl- β -D-glucopyranosyl)thiourea (3).

Method A: In an inert atmosphere, 4-fluorobenzylamine (1.25 g) was slowly added dropwise via syringe over 5 minutes at room temperature to a solution of glucose isothiocyanate **2** (3.89 g) in anhydrous CH_2Cl_2 (10 ml). The resulting mixture was stirred for 6 hours, and the progress of the reaction was monitored using thin-layer chromatography. The solvent was evaporated and the crude product was purified through silica gel column chromatography, using a mixture of ethyl acetate and hexane to afford pure **3** as light-yellow crystals, Yield: 79 %; m.p. 79 -81 °C.

Method B: A mixture of the corresponding 4-fluorobenzylamine (2 mmol) and tetra-O-acetyl- β -D-glucopyranosyl isothiocyanate (2 mmol) was gently ground in dry dioxane (3-5 mL) and subjected to microwave reflux for 12 minutes. The mixture transformed into a yellow paste. The solvent was evaporated and the crude product was purified through silica gel column chromatography, using a mixture of ethyl acetate and hexane to afford **3** in 89 % yield. IR (ν , cm^{-1}): 3449-3268 (2NH), 3037 (CH aromatic), 1754 (C=O), 1615 (C=N), 1370 (C=S); ^1H NMR (DMSO- d_6 , ppm): δ 2.05-2.10 (s, 12H, 4 CH_3CO), 3.95 (dd, $J = 5.2$ Hz, $J = 4.4$ Hz, 1H), 4.1 (m, 1H), 4.32-4.36 (dd, $J = 7.6$ Hz, $J = 4.8$ Hz, 1H), 4.88 (t, $J = 9.4$ Hz, 1H), 5.11 (t, $J = 10.0$ Hz, 1H), 5.37 (t, $J = 9.6$ Hz, 1H), 5.45 (d, 2H, benzylic), 5.73 (t, $J = 8.4$ Hz, 1H), 7.44 (d, $J = 2.4$ Hz, 2H, aromatic), 7.78 (d, $J = 8.4$ Hz, 2H, aromatic), 9.32 (br, 1H, NH), 11.97 (s, 1H, NH). ^{13}C NMR (DMSO- d_6 , ppm): δ : 20.62, 20.64, 20.72, 20.79, 61.70, 68.35, 70.82, 72.74, 73.49, 82.96, 127.94, 128.93, 169.74, 169.93, 170.85. Anal. calc. for $\text{C}_{22}\text{H}_{27}\text{FN}_2\text{O}_9\text{S}$ (514.52): C, 51.36; H, 5.29; F, 3.69; N, 5.44; O, 27.99; S, 6.23. Found C, 51.40; H, 5.27; F, 3.71; N, 5.41; O, 27.97; S, 6.24.

(Z)-3-(4-Fluorobenzyl)-2-(2',3',4', 6'- tetra-O-acetyl- β -D-glucopyranosyl-1'-imino)thiazolidin-4-one (4) and (Z)-2-(4-Fluorobenzylimino)-3-(2',3',4', 6'- tetra-O-acetyl- β -D-glucopyranosyl)thiazolidin-4-one (4').

A solution containing the corresponding thiourea derivative **3** (10 mmol) and anhydrous sodium acetate (0.82 g, 10 mmol) in ethanol (20 ml) or glacial acetic acid (15 ml) was prepared. To this solution, ethyl bromoacetate (2.5 g, 15 mmol) was added. The reaction mixture was refluxed for 12 hours. Then, the solvent was evaporated, and 20 mL of water was added. The resulting precipitate was filtered and then crystallized from a mixture of ethanol and water to afford isomeric mixture **4/4'** in the ration of 53 %: 47 %.

Yield 59 %; m.p. 150–152 °C, IR (KBr, cm^{-1}): ν 1752, 1740, 1591, 1577, 1567, 1513, 1237, 1032. **Isomer (4):** ^1H NMR (DMSO- d_6 , ppm): δ 1.91-2.1 (4s, 12H, 4(CH_3CO), 3.88 (s, 2H, S- CH_2), 3.98 (m, 1H), 4.01 (dd, $J = 5.2$ Hz, $J = 4.4$ Hz, 1H), 4.35 (dd, $J = 7.6$ Hz, $J = 4.8$ Hz, 1H), 5.01 (t, $J = 8.4$ Hz, 1H), 5.37 (t, $J = 10.0$ Hz, 1H), 5.45 (s, 2H, benzylic), 5.92 (t, $J = 8.4$ Hz, 1H, H-2), 6.35 (d, $J = 9.4$ Hz, 1H, H-1), 7.18 (d, $J = 2.4$ Hz, 2H, aromatic), 7.58 (d, $J = 8.4$ Hz, 2H, aromatic). ^{13}C NMR (DMSO- d_6 , ppm): δ : 28.85, 29.03, 29.08, 29.15, 30.6, 44.0, 64.0, 69.8, 73.7, 73.9, 76.3, 89.2, 118.91, 125.21, 129.52, 132.71, 153.4 (N=C-S), 160.9 (C-F), 168.9, 169.9, 170.3, 170.5, 171.01.

Isomer (4') : ^1H NMR (400MHz, DMSO- d_6 , ppm): δ 1.91-2.1 (4s, 12H, 4(CH_3CO)), 3.88 (s, 2H, S- CH_2), 3.98 (dd, $J = 5.2$ Hz, $J = 4.4$ Hz, 1H), 4.1 (m, 1H), 4.35 (dd, $J = 7.6$ Hz, $J = 4.8$ Hz, 1H), 5.01 (t, $J = 8.4$ Hz, 1H), 5.37 (t, $J = 10.0$ Hz, 1H), 5.45 (s, 2H, benzylic), 5.96 (d, $J = 9.4$ Hz, 1H, H-1), 6.44 (t, $J = 10$ Hz, 1H, H-2), 7.18 (d, $J = 2.4$ Hz, 2H, aromatic), 7.58 (d, $J = 8.4$ Hz, 2H, aromatic). ^{13}C NMR (DMSO- d_6 , ppm): δ 28.85, 29.03, 29.08, 29.15, 30.6, 44.0, 64.0, 69.8, 73.7, 73.9, 76.3, 89.2, 118.91, 125.21, 129.52, 132.71, 153.4, 160.9, 168.9, 169.9, 170.3, 170.5, 171.01.

2-Chloro-N-(4-fluorobenzyl)acetamide. [39]

A solution of 4-fluorobenzyl amine (1 equivalent) in 20 mL of dichloromethane was maintained at 0°C, and chloroacetyl chloride (1.5 equivalents) was slowly added with continuous stirring. The reaction mixture was then brought to room temperature and stirred for 4 hours. Crushed ice was added to the mixture and stirred vigorously. Ethyl acetate (EtOAc) was added, and the organic layer was washed with 1M HCl, a saturated NaHCO_3 solution, and NaCl. Then, it was separated, dried with Na_2SO_4 , filtered, and concentrated under vacuum. The crude product was further purified through silica gel column

chromatography, using a mixture of ethyl acetate and petroleum ether as the eluent, resulting in the isolation of 2-chloro-*N*-(4-fluorobenzyl)acetamide. as white solid, m.p. 112-114 °C, yield 85 %. ¹HNMR (CDCl₃ ppm): δ, 4.13 (s, 2H), 4.51 (d, *J* = 5.8 Hz, 2H), 7.00-7.11 (m, 2H, Ar), 7.26-7.33 (m, 2H, Ar).

(Z)-3-(4-Fluorobenzyl)-2-(2',3',4', 6'- tetra-O-acetyl-β-D-glucopyranosyl-1'- imino)thiazolidin-4-one (4).

2-Chloro-*N*-(4-fluorobenzyl)acetamide (1 mmol) and potassium carbonate (1.5 mmol) were added to a stirred solution in acetonitrile (5 ml). The addition of 2,3,4,6-tetra-*o*-acetyl-β-D-glucoseisothiocyanate (1 mmol) was completed over approximately 5 minutes. The reaction mixture was further stirred at room temperature for the necessary duration. The solvent was removed under reduced pressure, and the residue was subsequently purified through column chromatography, employing a mixture of petroleum ether and ethyl acetate (4:1) as the eluent. Yield: (72 %). m.p. 166-168°C; IR (ν, cm⁻¹): 2977, 2936 (CH aliphatic), 1726 (C=O), 1617 (C=N); ¹HNMR (DMSO-d₆ ppm): δ (4s, 12H, 4CH₃CO), 3.88 (s, 2H, S-CH₂), 3.98 (m, 1H), 4.01 (dd, *J* = 5.2 Hz, *J* = 4.4 Hz, 1H), 4.35 (dd, *J* = 7.6Hz, *J* = 4.8Hz, 1H), 5.01 (t, *J* = 8.4 Hz, 1H), 5.37 (t, *J* = 10.0 Hz, 1H), 5.45 (s, 2H, benzylic), 5.92 (t, *J* = 10 Hz, 1H), 6.35 (d, *J* = 9.4Hz, 1H), 7.18 (d, *J* = 2.4 Hz, 2H, aromatic), 7.58 (d, *J* = 8.4 Hz, 2H, aromatic). ¹³CNMR (DMSO-d₆, ppm): δ 28.85, 29.03, 29.08, 29.15 (4C-CH₃), 30.6 (S-CH₂), 44.0 (C-CH₂-N), 64.0 (O-CH₂), 69.8, 73.7, 73.9, 76.3 (4C), 89.2 (O-CH-N), 118.91 (2C), 125.21, 129.52 (2C) (Aromatic ring), 132.71 (C-CH₂-N), 153.4 (N=C-S), 160.9 (C-F), 168.9, 169.9, 170.3, 170.5, 171.01 (C=O). m/e: 554.14 (100.0 %), 555.14 (27.4%), 556.14 (5.8%), 556.13 (4.5%), 557.14 (1.8%). Anal. calc. for C₂₄H₂₇FN₂O₁₀S (554.54): C, 51.98; H, 4.91; F, 3.43; N, 5.05; O, 28.85; S, 5.78. Found C, 52.08; H, 4.88; F, 3.53; N, 5.44; O, 28.90; S, 5.17.

General procedure for the preparation of 5(a-f).

Compound 4 (0.277 g, 0.5 mmol) and the corresponding aromatic aldehyde (0.6 mmol) were dissolved in a mixture of ethanol and piperidine (30:1) and refluxed for 4–12 hours. After the reflux, the reaction mixture was allowed to cool. The resulting precipitated product was filtered and subsequently crystallized from a solvent mixture of ethanol and acetone (3:2).

(Z)-2-(4-Fluorobenzyl)-3-((Z)-4-(methoxy)benzylidene)-5-((2,3,4,6-tetra-*o*-acetyl-β-D-glucopyranosyl)imino) thiazolidin-4-one (5a).

Yield (95%); m.p. 167°C; IR (ν, cm⁻¹): 3524 (CH-Ar), 2857, 2928 (CH aliph.), 1734 (C=O), 1589 (C=N). ¹HNMR (DMSO-d₆, ppm): δ 2.05-2.1 (4s, 12H, 4CH₃CO), 3.73 (s, 3H, O-CH₃), 3.98 (m, 1H), 4.01 (dd, *J*=5.2 Hz, *J*=4.4 Hz, 1H), 4.35 (dd, *J* = 7.6Hz, *J*=4.8Hz, 1H), 5.01 (t, *J* = 8.4 Hz, 1H), 5.37 (t, *J* = 10.0 Hz, 1H), 5.45 (s, 2H, benzylic), 5.92 (t, *J* = 10 Hz, 1H), 6.35 (d, *J* = 9.4 Hz, 1H), 6.76 (d, *J* = 8.8 Hz, 2H aromatic), 7.07 (d, *J* = 8.4Hz, 2H aromatic), 7.38 (d, *J* = 8.8 Hz, 2H aromatic), 7.46 (d, *J* = 8.4 Hz, 2H aromatic), 7.74 (s, 1H, S-C=CH). ¹³C NMR (DMSO-d₆, ppm): δ 28.85, 29.03, 29.08, 29.15 (4C-CH₃), 55.6 (O-CH₃), 44.0 (C-CH₂-N), 64.0 (O-CH₂), 69.8, 73.7, 73.9 (1C), 102.9 (O-C-N), 111.1(2C), 118.9 (2C), 125.3, 129.6, 129.5, 132.2 (2C) (Aromatic ring), 132.7 (C-CH₂-N), 145.6 (S-C=CH-), 154.5 (N=C-S), 160.9 (C-F), 168.9, 169.9, 170.3, 170.5, 171.01 (C=O). m/e: 672.18 (100.0%), 673.18 (36.6%), 674.19 (6.1%), 674.17 (4.5%), 674.18 (2.8%), 675.18 (1.7%), 675.19 (1.5%). LC-MS: m/z calcd. for C₃₂H₃₃FN₂O₁₁S (672.18); found, 672.85 [M + H]⁺, 690.40 [M + H₂O]. Anal. calc. for C₃₂H₃₃FN₂O₁₁S (672.67): C, 57.14; H, 4.94; F, 2.82; N, 4.16; O, 26.16; S, 4.77. Found: C, 57.11; H, 4.90; F, 2.84; N, 4.11; O, 26.29; S, 4.75.

(Z)-2-(4-Fluorobenzyl)-3-((Z)-4-chlorobenzylidene)-5-((2,3,4,6-tetra-*o*-acetyl-β-D-glucopyranosyl)imino) thiazolidin-4-one (5b).

Yield (95%); m.p. 160°C; IR (ν, cm⁻¹): 3409 (CH-Ar), 2820, 2890 (CH aliph.), 1710 (C=O), 1595 (C=N). ¹HNMR (400MHz, DMSO-d₆, ppm): δ 2.05-2.1 (4s, 12H, 4CH₃CO), 3.98 (m, 1H), 4.01 (dd, *J* = 5.2 Hz, *J* = 4.4 Hz, 1H), 4.35 (dd, *J* = 7.6Hz, *J* = 4.8Hz, 1H), 5.01 (t, *J* = 8.4 Hz, 1H), 5.37 (t, *J* = 10.0 Hz, 1H), 5.45 (s, 2H, benzylic), 5.92 (t, *J* = 10 Hz, 1H), 6.35 (d, *J* = 9.4 Hz, 1H), 6.76 (d, *J* = 8.8 Hz, 2H aromatic), 7.07 (d, *J* = 8.4Hz, 2H aromatic), 7.46 (d, *J* = 8.4 Hz, 2H aromatic), 7.74 (s, 1H, S-C=CH). ¹³C NMR (DMSO-d₆, ppm): δ 28.85, 29.03, 29.08, 29.15 (4C-CH₃), 44.0 (C-CH₂-N), 64.0 (O-CH₂), 69.8, 73.7, 73.9 (1C), 102.9 (O-C-N), 111.1 (2C), 118.9 (2C), 125.3, 129.5, 129.5, 132.2 (2C), (Aromatic ring), 132.7 (C-CH₂-N), 145.7 (S-C=CH-), 154.5 (N=C-S), 160.9 (C-F), 168.9, 169.9, 170.3, 170.5, 171.01 (C=O). m/e: 676.13 (100.0%), 678.13 (39.1%), 677.13 (35.4%), 679.13 (12.8%), 678.14

(5.7%), 680.13 (3.0%), 680.12 (1.5%), 679.14 (1.4%). Anal. calc. for $C_{31}H_{30}ClFN_2O_{10}S$ (677.09): C, 54.99; H, 4.47; Cl, 5.24; F, 2.81; N, 4.14; O, 23.63; S, 4.74. Found: C, 54.95; H, 4.42; Cl, 5.29; F, 2.81; N, 4.16; O, 23.65; S, 4.72.

(Z)-2-(4-Fluorobenzyl)-3-((Z)-4-(hydroxy-3-methoxy)benzylidene)-5-((2,3,4,6-tetra-o-acetyl- β -D-glucopyranosyl) imino) thiazolidin-4-one (5c).

Yield (95%); m.p. 169°C; IR (ν , cm^{-1}): 3336-3452 (CH-Ar), 3343(OH broadband), 2887, 2816 (CH aliph.), 1644 (C=O), 1590 (C=N). 1H NMR (DMSO- d_6 , ppm); δ 2.05-2.1 (4s, 12H, 4CH₃CO), 3.73 (s, 3H, O-CH₃), 3.98 (m, 1H), 4.01 (dd, J = 5.2 Hz, J = 4.4 Hz, 1H), 4.35 (dd, J = 7.6Hz, J = 4.8Hz, 1H), 5.01 (t, J = 8.4 Hz, 1H), 5.37 (t, J = 10.0 Hz, 1H), 5.45 (s, 2H, benzylic), 5.92 (t, J = 10 Hz, 1H), 6.35 (d, J = 9.4 Hz, 1H), 6.76 (d, J = 8.8 Hz, 2H aromatic), 7.07 (d, J = 8.4 Hz, 2H aromatic), 7.38 (d, J = 8.8 Hz, 2H aromatic), 7.46 (d, J = 8.4 Hz, 2H aromatic), 7.74 (s, 1H, S-C=CH), 9.81(s, 1H, OH). ^{13}C NMR (DMSO- d_6 , ppm); δ 20.7, 21.0, 21.0, 21.1 (-CH₃), 56.2 (O-CH₃), 44.0 (C-CH₂-N), 64.0 (O-CH₂), 69.8, 73.7, 73.9 (1C), 102.9 (O-C-N), 112.0, 115.3, 115.3, 116.8, 120.1, 128.6, 128.6, 128.8, 137.3, 144.9, 151.3, 160.9, 145.7 (S-C=CH-), 154.5 (N=C-S), 160.9 (C-F), 168.9, 169.9, 170.3, 170.5, 171.01 (C=O). m/e: 688.17 (100.0%), 689.18 (35.4%), 690.18 (8.9%), 690.17 (4.8%), 691.18 (1.7%), 691.17 (1.6%), 689.17 (1.5%). Anal. calc. for $C_{32}H_{33}FN_2O_{12}S$ (688.67): C, 54.22; H, 5.04; F, 1.86; N, 2.75; O, 32.97; S, 3.15. Found: C, 54.12; H, 5.07; F, 1.91; N, 2.73; O, 32.90; S, 3.11.

(Z)-2-(4-Fluorobenzyl)-3-((Z)-4-(dimethylamino)benzylidene)-5-((2,3,4,6-tetra-o-acetyl- β -D-glucopyranosyl) imino) thiazolidin-4-one (5d).

Yield (95%); m.p. 167–170 °C; IR (ν , cm^{-1}): 3108-3019 (CH-Ar), 2929, 2864 (CH aliph.), 1726 (C=O), 1599(C=N). 1H NMR (400MHz, DMSO- d_6 , ppm); 2.05-2.1 (4s, 12H, 4CH₃CO), 2.85 (s, 6H, N-Me₂), 3.98 (m, 1H), 4.01 (dd, J = 5.2 Hz, J = 4.4 Hz, 1H), 4.35 (dd, J = 7.6Hz, J = 4.8Hz, 1H), 5.01 (t, J = 8.4 Hz, 1H), 5.37 (t, J = 10.0 Hz, 1H), 5.45 (s, 2H, benzylic), 5.92 (t, J = 10 Hz, 1H), 6.35 (d, J = 9.4 Hz, 1H), 6.76 (d, J = 8.8 Hz, 2H aromatic), 7.07 (d, J = 8.4Hz, 2H aromatic), 7.38 (d, J = 8.8 Hz, 2H aromatic), 7.46 (d, J = 8.4 Hz, 2H aromatic), 7.74 (s, 1H, S-C=CH). ^{13}C NMR (DMSO- d_6 , ppm); δ 20.7, 21.0, 21.0, 21.1 (-CH₃), 40.1, 40.9 (N-Me₂), 44.0 (C-CH₂-N), 64.0 (O-CH₂), 69.9, 73.7, 73.9 (1C), 102.9

(O-C-N), 111.1, 111.1, 118.9, 118.9, 125.3, 129.6, 129.5, 132.2, 132.2 (Aromatic ring), 132.7 (C-CH₂-N), 145.7 (S-C=CH-), 154.5 (N=C-S), 160.9 (C-F), 168.9, 169.9, 170.3, 170.5, 171.01 (C=O). m/e: 685.21 (100.0%), 686.21 (38.0%), 687.21 (7.3%), 687.22 (6.5%), 688.21 (1.8%), 688.22 (1.5%). Anal. calc. for $C_{33}H_{36}FN_3O_{10}S$ (685.72): C, 57.80; H, 5.29; F, 2.77; N, 6.13; O, 23.33; S, 4.68. Found: C, 57.77; H, 5.22; F, 2.74; N, 6.11; O, 23.32; S, 4.84.

(Z)-2-(4-Fluorobenzyl)-3-((Z)-4-(p-nitro)benzylidene)-5-((2,3,4,6-tetra-o-acetyl- β -D-glucopyranosyl) imino) thiazolidin-4-one (5e).

Yield (95%); m.p. 170°C; IR (ν , cm^{-1}): 3120-3112 (CH-Ar), 2910, 2860 (CH aliph.), 1710 (C=O), 1619 (C=N). 1H NMR (400MHz, DMSO- d_6 , ppm) δ 2.05-2.1 (4s, 12H, 4CH₃CO), 3.98 (m, 1H), 4.01 (dd, J = 5.2 Hz, J = 4.4 Hz, 1H), 4.35 (dd, J = 7.6Hz, J = 4.8Hz, 1H), 5.01 (t, J = 8.4 Hz, 1H), 5.37 (t, J = 10.0 Hz, 1H), 5.45 (s, 2H, benzylic), 5.92 (t, J = 10 Hz, 1H), 6.35 (d, J = 9.4 Hz, 1H), 6.76 (d, J = 8.8 Hz, 2H aromatic), 7.07 (d, J = 8.4Hz, 2H aromatic), 7.36 (d, J = 8.8 Hz, 2H aromatic), 7.46 (d, J = 8.4 Hz, 2H aromatic), 7.74 (s, 1H, S-C=CH). ^{13}C NMR (DMSO- d_6 , ppm); δ 28.85, 29.03, 29.08, 29.15 (4C-CH₃), 44.0 (C-CH₂-N), 64.0 (O-CH₂), 69.8, 73.7, 73.9 (1C), 102.9 (O-C-N), 111.1 (2C), 118.9 (2C), 125.2, 129.6, 129.5, 132.2(2C) (Aromatic ring), 132.7 (C-CH₂-N), 145.7 (S-C=CH-), 154.5 (N=C-S), 160.9 (C-F), 168.9, 169.9, 170.3, 170.5, 171.01 (C=O). m/e: 191.92 (100.0%), 193.92 (4.5%), 193.93 (2.1%). Anal. calc. for $C_{31}H_{30}FN_2NO_2O_{10}S$ (1159.64): C, 32.11; H, 2.61; F, 1.64; N, 2.42; No, 44.67; O, 13.80; S, 2.77. Found: C, 32.14; H, 2.55; F, 1.67; N, 2.48; No, 44.65; O, 13.79; S, 2.72.

(Z)-2-(4-Fluorobenzyl)-3-((Z)-4-biphenylcarboxalidene)-5-((2,3,4,6-tetra-o-acetyl- β -D-glucopyranosyl) imino) thiazolidin-4-one (5f).

Yield (95%); m.p. 163–164°C; IR (ν , cm^{-1}): 2935, 2843 (CH aliph.), 1704 (C=O), 1618 (C=N). 1H NMR (DMSO- d_6 , ppm) δ 2.05-2.1 (4s, 12H, 4CH₃CO), 3.98 (m, 1H), 4.01 (dd, J = 5.2 Hz, J = 4.4 Hz, 1H), 4.35 (dd, J = 7.6Hz, J = 4.8Hz, 1H), 5.01 (t, J = 8.4 Hz, 1H), 5.37 (t, J = 10.0 Hz, 1H), 5.45 (s, 2H, benzylic), 5.92 (t, J = 10 Hz, 1H), 6.35 (d, J = 9.4 Hz, 1H), 6.76 (d, J = 8.8 Hz, 2H aromatic), 6.85 (d, J = 8.8Hz, 2H aromatic), 7.22 (t, 1H aromatic), 7.32 (d, J = 8.4Hz, 2H aromatic), 7.36 (d, J = 8.4 Hz, 2H aromatic), 7.43 (d, J = 8.4 Hz, 2H aromatic), 7.48 (d, J = 8.1 Hz, 2H aromatic), 7.74 (s, 1H, S-C=CH). ^{13}C NMR (DMSO- d_6 , ppm); δ 28.85, 29.03, 29.08,

29.15,44.0, 64.0, 69.9, 73.7, 73.9, 102.9,111.10, 111.12, 118.9 ,118.9, 125.3,126.9, 126.92, 127.6, 127.78, 127.79, 127.80, 127.81, 129.61, 129.62, 132.20, 132.21,132.7, 134.1, 135.7, 136.5, 137.3 ,145.7 (S-C=CH-), 154.5 (N=C-S), 160.9 (C-F), 168.9, 169.9, 170.3, 170.5, 171.01 (C=O). m/e: 718.20 (100.0%), 719.20 (41.9%), 720.21 (8.1%), 720.20 (7.2%), 721.21 (1.9%), 721.20 (1.9%). Anal. calc. for C₃₇H₃₅FN₂O₁₀S (718.74): C, 61.83; H, 4.91; F, 2.64; N, 3.90; O, 22.26; S, 4.46. Found: C, 61.84; H, 4.87; F, 2.61; N, 3.95; O, 22.23; S, 4.50.

General procedure for the synthesis of compounds **6c** and **6d**.

A saturated solution of ammonia in methanol (30 ml) was added to a solution containing the respective compounds **5c** or **5d** (10 mmol) in dry methanol (10 ml). The mixture was stirred at room temperature for 24 hours. Subsequently, the liquid ammonia was allowed to evaporate. The remaining residue was dissolved in 20 ml of warm methanol. This solution was then filtered, and the filtrate was subjected to evaporation under reduced pressure. The solution was filtered, and the filtrate was evaporated under reduced pressure and dried under vacuum to afford the deacylated product **6c** and **6d**.

(Z)-2-(4-Fluorobenzyl)-3-((Z)-4-(hydroxy-3-methoxy)benzylidene)-5-((β-D-glucopyranosyl)imino)thiazolidin-4-one (**6c**).

Yield (72 %), IR (ν, cm⁻¹): 3593 (-OH), 3336-3452 (CH-Ar), 2816, 2887 (CH aliph.), 1644 (C=O), 1590 (C=N). ¹HNMR (400MHz, DMSO-d₆, ppm); δ: 3.73 (s, 3H, O-CH₃), 3.98 (m, 1H), 4.01 (dd, J=5.2 Hz, J=4.4 Hz, 1H), 4.35 (dd, J=7.6Hz, J=4.8Hz, 1H), 4.61 (d, J=5.5Hz, 1H, OH), 4.68 (t, J=5.6Hz, 1H, OH), 4.71 (d, J=5.5Hz, 1H, OH), 4.91 (d, J = 5.5Hz, 1H, OH), 5.01 (t, J = 8.4 Hz, 1H), 5.37 (t, J = 10.0 Hz, 1H), 5.45 (s, 2H, benzylic), 5.92 (t, J = 10 Hz, 1H), 6.35 (d, J = 9.4 Hz, 1H), 6.76 (d, J = 8.8 Hz, 2H aromatic), 7.07 (d, J = 8.4 Hz, 2H aromatic), 7.38 (d, J = 8.8 Hz, 2H aromatic), 7.36 (d, J = 8.4 Hz, 2H aromatic), 7.46 (d, J = 8.4 Hz, 2H aromatic), 7.74 (s, 1H, S-C=CH). 9.81 (s, 1H, OH). m/e: 520.13 (100.0%), 521.13 (27.5%), 522.14 (5.0%), 522.13 (4.9%), 523.13 (1.2%). Anal. calc. for C₂₄H₂₅FN₂O₈S (520.53): C, 55.38; H, 4.84; F, 3.65; N, 5.38; O, 24.59; S, 6.16. Found: C, 55.11; H, 5.04; F, 3.17; N, 5.33; O, 25.09; S, 6.26.

(Z)-2-(4-Fluorobenzyl)-3-((Z)-4-(dimethylamino)benzylidene)-5-((β-D-glucopyranosyl)imino)thiazolidin-4-one (**6d**).

Yield (64%). IR (ν, cm⁻¹): 3448 (-OH), 3108-3019 (CH-Ar), 2929, 2864 (CH aliph.), 1726 (C=O), 1599 (C=N). ¹HNMR (DMSO-d₆, ppm); 2.85 (s, 6H, N-Me₂), 3.98 (m, 1H), 4.01 (dd, J = 5.2 Hz, J = 4.4 Hz, 1H), 4.35 (dd, J = 7.6Hz, J = 4.8Hz, 1H), 4.63 (d, J = 5.5Hz, 1H, OH), 4.68 (t, J = 5.6Hz, 1H, OH), 4.71 (d, J = 5.5Hz, 1H, OH), 4.90 (d, J = 5.5Hz, 1H, OH), 5.01 (t, J = 8.4 Hz, 1H), 5.37 (t, J = 10.0 Hz, 1H), 5.45 (s, 2H, benzylic), 5.92 (t, J = 10 Hz, 1H), 6.35 (d, J = 9.4 Hz, 1H), 6.76 (d, J = 8.8 Hz, 2H aromatic), 7.07 (d, J = 8.4Hz, 2H aromatic), 7.46 (d, J = 8.4 Hz, 2H aromatic), 7.74 (s, 1H, S-C=CH). m/e: 517.17 (100.0%), 518.17 (29.5%), 519.17 (5.3%), 519.16 (4.5%), 520.17 (1.3%). Anal. calc. for C₂₅H₂₈FN₃O₆S (517.57): C, 58.01; H, 5.45; F, 3.67; N, 8.12; O, 18.55; S, 6.70. Found: C, 57.81; H, 5.40; F, 3.60; N, 7.92; O, 18.51; S, 6.26.

2.2 In Vitro Acetyl-Cholinesterase Enzyme Inhibition Assay

The acetylcholinesterase activity was assessed using QuantiChrom™ Screening Kit (IACE-100) obtained from BioAssay Systems. Three positive controls; Donepezil, Tacrine and Rivastagmine were tested alongside the **8** synthesized compounds, following the kit's instructions. A dose-response curve was generated by performing serial logarithmic dilutions (10 - 1000 nM) of all the tested compounds, and IC₅₀ values were calculated from the curve.

2.3 Molecular docking

2.3.1 Receptor preparation

The protein sequence data of hAChE was obtained from the protein data bank (PDB) with the ID 4EY7. The selected PDB file was prepared using MOE v.2019.01 with the AMBER10: EHT forcefield. The preparation steps included adding 3D protonation, deleting water molecules that were more than 4.5 Å away from the complex, and refining the structure to 0.1 kcal/mol/Å.

2.3.2 Ligand preparation

The MDL molfiles of the 8 designed compounds (**5a-f**, **6c** and **6d**) were drawn using ChemDraw 18.0. The ligand files was then opened in a new database to convert chemical formats. Hydrogen atoms were added to the ligands using the Add hydrogen option, partial charges and energy minimize also done for the ligands.

2.3.3 Docking

Docking is a molecular modeling technique that is used to predict how a protein interacts with ligands. MOE 2015, a software for molecular modeling and simulation, was used to redock the co-crystallized ligand to validate the docking parameters. Then, the 8 synthesized compounds were docked on the ligand binding site using the triangle matcher placement method, London dG scoring function, and force field refinement was accomplished on the top 5 poses per each compound.

3. Results and Discussion

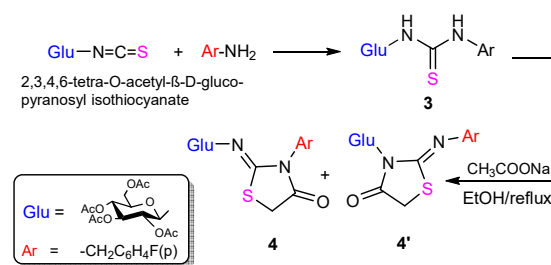
Thiadiazolidin-4-one, known for its unique five-membered ring structure with sulfur, nitrogen, and a carbonyl group, has gained attention in medicinal chemistry. Its derivatives are studied for anti-inflammatory, antioxidant, and antimicrobial properties, sparking interest in both chemistry and biology. To achieve the title compound, we initiate the process with the synthesis of 2,3,4,6-tetra-O-acetyl- β -D-glucopyranosyl isothiocyanate from refluxing α -bromoacetoglucose with an excess of $\text{Pb}(\text{SCN})_2$ in hot dry toluene [36].

The later compound was subjected to react with 4-fluorobenzylamine to afford 1-(4-fluorobenzyl)-3-(2,3,4,6-tetra-o-acetyl- β -D-glucopyranosyl) thiourea **3**. This reaction was carried in two distinct procedures. In the first approach, the reaction occurred under inert atmospheric conditions, utilizing anhydrous CH_2Cl_2 as the solvent, followed by stirring at room temperature for a duration of 3 hours. Conversely, the second procedure involved the use of a microwave oven, significantly reducing the reaction time to a matter of minutes.

Notably, the nucleophilic addition of 4-fluorobenzylamine to the sugar isothiocyanate proceeded smoothly in both methods. Interestingly, the second method yielded a higher product yield, reaching 89 %, as compared to the first method, which yielded 79 %. Additionally, the second approach exhibited environmental friendliness as an added advantage.

The structure of glucopyranosyl thiourea **3** was established through elemental analysis and spectral data. The IR spectra clearly indicated the presence of strong carbonyl absorption bands at 1754 cm^{-1} , NH absorption between 3449 and 3268 cm^{-1} , and C=S absorption at 1370 cm^{-1} , as detailed in the experimental section. In the $^1\text{H-NMR}$ spectrum,

distinct resonance signals emerged at δ 9.32 and 11.97 ppm, corresponding to the thiourea N–H protons. Furthermore, the C–H protons within the pyranose ring of the monosaccharides displayed chemical shifts spanning from δ 5.73 ppm to 3.95 ppm, consistent with the typical $^1\text{H-NMR}$ spectra observed in monosaccharide compounds. It's worth noting that proton H-1 of the glucopyranose ring appeared as a triplet at approximately δ 4.88 ppm with a coupling constant of $J = 9.4\text{ Hz}$, while the resonance signal of proton H-2 appeared as a triplet at δ 5.11 ppm with a coupling constant of $J = 10.0\text{ Hz}$. These coupling constants provide evidence supporting the β -anomer configuration for the NH-thiourea group due to trans-H–H coupling interactions.



Scheme 1: Cyclization of glycosyl thiourea **3** with ethylbromoacetate

The resulting thiourea derivative was then subjected to an $\text{S}_{\text{N}}2$ nucleophilic substitution reaction with 3.0 equivalents of ethyl bromoacetate and 2.0 equivalents of NaOAc in EtOH under reflux for 12–20 hours. This reaction produced a 1:1 mixture of isomeric iminothiazolidinone products, **4** and **4'**, with an overall yield of 59 %. Separating these isomers proved challenging due to low their stereoselectivity, even after experimenting with different solvents, temperatures, and excess ethyl bromoacetate. In the case of isomer **4**, both of glucopyranose and the benzyl moiety occupy positions 3 and 2 within the thiazolidine ring, forming either a direct bond with the nitrogen atom or an imino bond, respectively. In contrast, for isomer **4'**, these moieties are found at positions 2 and 3 of the thiazolidine ring. Due to these structural similarities shared between **4** and **4'**, the separation of these isomers using methods like recrystallization or column chromatography are unfeasible. All attempts from changing experimental conditions like solvent, time, heat, increasing or decreasing amount of ethyl bromoacetate to obtain one regioisomeric iminothiazolidinone product failed.

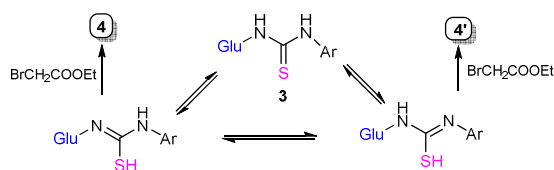
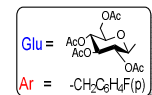
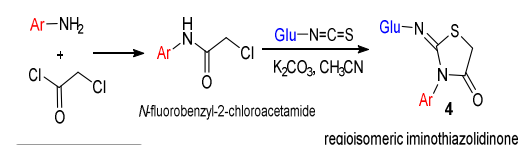


Figure 3: The tautomeric forms of glycosyl thiourea derivative **3** during its reaction with ethylbromoacetate

The formation of the diastereomeric products **4** and **4'** was confirmed based on the analysis of their ^1H NMR spectra, as presented in the experimental section. The formation of diastereomeric products **4** and **4'** can be anticipated, attributed to the presence of tautomeric forms of thiourea in equilibrium. This equilibrium suggests that the sulfur atom in the thiol-tautomer acts as a nucleophile when reacting with ethyl bromoacetate (Fig. 3).



Scheme 2: Cyclization of *N*-fluorobenzyl-2-chloroacetamide with glucoseisothiocyanate

To achieve our goal of preparing one regioisomeric iminothiazolidinone derivative from suagr isothiocyanate, we devised an alternative route. First, we reacted 4-fluorobenzylamine with chloroacetyl chloride, resulting in the formation of *N*-fluorobenzyl-2-chloroacetamide. Subsequently, this compound underwent a smooth reaction with a solution of 2,3,4,6-tetra-*O*-acetyl- β -*D*-glucose isothiocyanate in CH_3CN , in the presence of K_2CO_3 as a weak base. Given the ambident nucleophilic nature of isothiocyanate, it is possible to consider two distinct end structures for the heterocycles: either thiohydantoin or iminothiazolidinone, as depicted in Scheme 3.

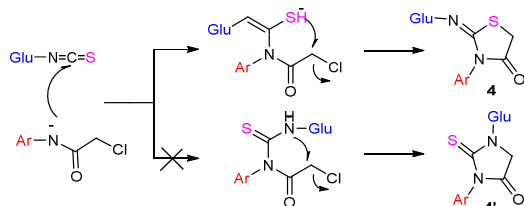
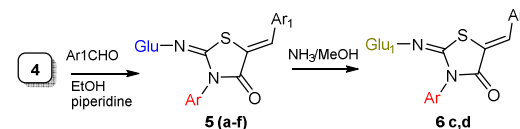


Figure 4: Postulated mechanism for the formation of **4** or **4'**

The spectroscopic data indicates that the chlorine atom has been replaced by the nucleophile, and a cyclization has occurred. Both thiohydantoin and iminothiazolidinone structures are in line with these observations. However, classical spectroscopic data does not definitively establish which compound has been precisely formed. Hence, additional efforts were undertaken to confirm the structural identity.

I made several attempts to utilize X-ray analysis for three-dimensional single crystal analysis, but unfortunately, all of these attempts were unsuccessful. The identification of the novel product structure relied on their microanalytical and spectroscopic data (^1H NMR, ^{13}C NMR, and IR). The preference for the **4** structure over the isomeric **4'** is substantiated by several factors. These include analysis of the ^{13}C NMR spectra, a comparison with previously reported data in the literature [40-45], and X-ray structural analysis of similar structures documented in literature references [46].



(a): $\text{Ar}_1 = \text{C}_6\text{H}_4\text{OMe}$ (4) (b): $\text{Ar}_1 = \text{C}_6\text{H}_4\text{Cl}$ (4) (c): $\text{Ar}_1 = 4(\text{OH})\text{C}_6\text{H}_3\text{-OMe}$
(d): $\text{Ar}_1 = \text{C}_6\text{H}_4\text{Me}_2\text{N}$ (4) (e): $\text{Ar}_1 = \text{C}_6\text{H}_4\text{O}_2\text{N}$ (4) (f): $\text{Ar}_1 = \text{C}_6\text{H}_5\text{C}_6\text{H}_4$



Scheme 3: Reaction of iminothiazolidinone and aldehyds followed by deprotection

Finally, the desired products **5(a-f)** were obtained through Knoevenagel condensation reaction between compound **4** and various aromatic aldehydes in a mixture of ethanol and piperidine under reflux (Scheme 3). The structures of the new products were established according to their microanalytical and spectroscopic data (see experimental)

Deprotection of compounds **5c** and **5d** using ammonia in methanol at room temperature resulted in the formation of the deacetylated products **6c** and **6d**. Infrared (IR) analysis revealed the presence of an OH group at 3448 cm^{-1} and an amidic CO group at 1734 cm^{-1} . Furthermore, the ^1H NMR spectrum exhibited no absorption signals for the acetyl protons, while the base protons were detected, as showed in the experimental data.

3.1. In Vitro Acetyl-Cholinesterase Enzyme Inhibition Assay and SAR

Acetylcholinesterase is an enzyme crucial for breaking down the neurotransmitter acetylcholine, and controlling its activity can be vital in treating conditions like Alzheimer's. To evaluate the potential of the seven synthesized compounds as candidates for Alzheimer's disease (AD) symptomatic treatment, an in vitro inhibition assay targeting acetylcholinesterase (AChE) was conducted. Employing Ellman's method spectrophotometer, the results were compared with three FDA-approved drugs known for their AChE inhibitory properties: donepezil, tacrine, and rivastigmine. The inhibitory concentration (IC_{50}) data, as presented in Fig. 3 and Table 1, provide valuable insights into the relative activity of these compounds. The inhibitory concentration (IC_{50}) data, presented in Fig. 3 and Table 1, reveals that compound **5a** exhibits the most potent AChE inhibition activity ($IC_{50} = 0.209 \mu\text{g/mL}$), approximately 13 times more active than rivastigmine ($IC_{50} = 2.765 \mu\text{g/mL}$) and roughly 2 times more active than Tacrine ($IC_{50} = 0.447 \mu\text{g/mL}$), as well as being comparable in activity to donepezil ($IC_{50} = 0.143 \mu\text{g/mL}$). Furthermore, compounds **5f**, **6c**, and **6d** displayed IC_{50} values of 0.286, 0.319 $\mu\text{g/mL}$, and 0.214 $\mu\text{g/mL}$, respectively. These compounds outperformed tacrine and rivastigmine, emphasizing their potential as promising candidates for AD treatment. In contrast, compounds **5b**, **5c**, and **5e** exhibited intermediate activity with IC_{50} values of 1.793, 0.91 and 1.395 $\mu\text{g/mL}$, respectively, all surpassing the activity of rivastigmine. The least potent derivatives were **5d** ($IC_{50} = 3.608 \mu\text{g/mL}$). These findings underscore the potential of certain synthesized compounds, particularly **5a**, **5f**, **6c**, and **6d**, for further exploration and development as promising candidates for symptomatic treatment in Alzheimer's disease. Further research and optimization are warranted to harness the therapeutic potential of these compounds effectively.

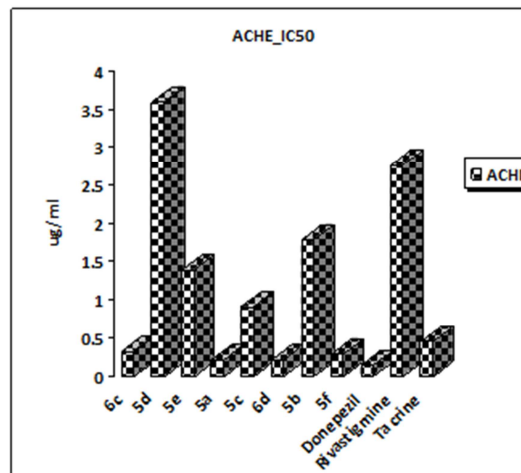


Figure 5: Statistical comparison of inhibitory concentration data (IC_{50} values) of 7 synthesized compounds, Donepezil, Tacrine, and Rivastigmine against AChE

Table 1. IC_{50} values of compounds **5a**, **5b**, **5c**, **5d**, **5e**, **5f**, **6c**, **6d**, Donepezil, Tacrine, and Rivastigmine against acetylcholinesterase (AChE)

Serial	Compound Number in Scheme	AChE	
		IC_{50} ($\mu\text{g/mL}$)	\pm SD*
1	5a	0.209	0.01
2	5b	1.793	0.07
3	5c	0.91	0.04
4	5d	3.608	0.14
5	5e	1.395	0.05
6	5f	0.286	0.01
7	6c	0.319	0.01
8	6d	0.214	0.01
*	Donepezil	0.143	0.01
**	Rivastigmine	2.765	0.11
***	Tacrine	0.447	0.02

* Experiments were run in triplicates and the data presented are the mean IC_{50} values \pm standard deviation

Structure-activity relationship

The structure-activity relationship presented here is derived from studies on acetylcholinesterase inhibitors (Figure 1). The various benzaldehyde substitutions employed in the synthesis of the final derivatives **5a-f**, **6c** and **6d** had a substantial effect on the function of acetylcholinesterase inhibition. For instance, Compound **5a**, having an electron-donating methoxy group ($-\text{OCH}_3$) on the phenyl ring, displays strong inhibitory activity, as reflected in its low IC_{50} value of 0.209 $\mu\text{g/mL}$. Conversely, Compound **5b**, which substitutes an electron-withdrawing chloro group ($-\text{Cl}$), exhibits reduced inhibitory potential with an IC_{50} value of 1.793 $\mu\text{g/mL}$ when compared to the

methoxy substitution. Compounds **5c**, with both hydroxy (-OH) and methoxy (-OCH₃) groups at positions **4** and **3**, respectively, demonstrate a moderate effect on inhibitory activity, indicated by their IC₅₀ values of 0.91 ug/ml. Compound **5d** introduces an N,N-dimethylamino group (-N(CH₃)₂) at the 4-position on the aryl (Ar) group, leading to significantly weaker inhibitory activity as evidenced by a higher IC₅₀ value. In Compound **5e**, the presence of a nitro group (-NO₂) at the 4-position on the aryl (Ar) group results in intermediate inhibitory activity, with an IC₅₀ value of 1.395 ug/ml. Additionally, Compound **5f** (Ar = biphenyl) displays strong inhibitory activity, with an IC₅₀ value of 0.286 ug/ml. The IC₅₀ values for both Compound **6c** (IC₅₀ = 0.319 ug/ml) and Compound **6d** (IC₅₀ = 0.214 ug/ml) underscore the significant impact of these specific substitutions on inhibitory activity. These findings highlight the significant influence that the choice of substituents on the aryl group has on the inhibitory capabilities of these compounds.

3.2. Molecular docking and *in silico* pharmacokinetics prediction

The drugs rivastigmine and tacrine, as well as compounds **5a-f**, **6c** and **6d**, were docked to the AChE active site (PDB ID: 4EY7). The validity of the docking method was verified by re-docking the co-crystallized ligand (donepezil) to the active site pocket. Each ligand-protein pair in **Table 2** exhibited a negative binding energy, indicating that recognition between the compounds of interest and the intended protein was thermodynamically advantageous. The p-methoxy phenyl and thiazolidine rings of compounds **5a** and **5b** were detected to have pi-pi stacking with Tyr 341 (Fig. 6). In addition to, **5b** revealed an arene-H contact with Phe 295. **5c** and **5d**

showed an H-bond with Tyr 341 amino acid. Further, **5d** established an H-arene interaction with the residue Trp 286. The interaction of **5e** against the target protein AChE was confirmed with Tyr 341 through an arene-H interaction, with Trp 286 and Tyr 341 through pi-pi stacking with thiazolidine and p-nitro phenyl rings, respectively. **5f** was combined with the receptor through two hydrogen bonds with Ser 293 and two H-arene bonds with Tyr 337 and Tyr 341 amino acids (Fig. 7). **6c** predicted binding pattern identified three hydrogen bonds with amino acid residues, including Glu 202, Gln 71 and Gly 122, as well as the p-fluorophenyl group was detected to have pi-pi stacking with Tyr 341 (Fig. 6). Compound **6d** stabilized the connection with AChE through forming two hydrogen bonds with the residues His 447 and Asp 74 (Fig. 9). Donepezil and rivastigmine were coupled with the receptor protein by forming an H-arene bond with Tyr 337 and Trp 86; respectively (Fig. 10,11). Finally, tacrine formed two H-arene contacts with Tyr 341 and Trp 86 amino acids (Fig. 12). After successful docking of the compounds (**5a-f**, **6c,d**) with AChE (PDB ID: 4EY7), the results showed significant interactions. The binding affinity docking score of the compounds (**5a-f**, **6c,d**) are -8.91 Kcal/mole, -6.71 Kcal/mole, -7.65 Kcal/mole, -8.04 Kcal/mole, -7.81 Kcal/mole, -8.76 Kcal/mole, -6.93 Kcal/mole, and -8.41 Kcal/mole, respectively (table 2). All the tested compounds showed binding affinity score higher than that of rivastigmine (-6.39 Kcal/mole) and tacrine (-5.77 Kcal/mole). Compounds **5a,f** and **6c,d** showed a docking score higher than or near to that of donepezil (-7.74 Kcal/mole) and this means that they have a lot of potential as bioactive compounds.

Table 2. Docking interaction data calculations of **5(a-f)**, **6(c,d)**, donepezil, rivastigmine and tacrine inside AChE (PDB ID: 4EY7) active spots

Compound	Binding affinity (Kcal/mol)	Affinity Bond strength (Kcal/mol)	Affinity Bond length (in Å° from the main residue)	Amino acids	Ligand	Interaction
5a	-8.91	-0.0	3.99	TYR 341	6-ring	pi-pi
5b	-6.71	-0.6 -0.0	3.76 3.88	PHE 295 TYR 341	6-ring 5-ring	pi-H pi-pi
5c	-7.65	-1.0	3.97	TYR 341	S 18	H-donor

5d	-8.04	-0.8	3.37	TYR 341	C 5	H-donor
		-1.4	3.88	TRP 286	C 12	H-pi
5e	-7.81	-0.7	4.32	TYR 341	5-ring	pi-H
		-0.0	3.97	TRP 286	5-ring	pi-pi
		-0.0	3.70	TYR 341	6-ring	pi-pi
5f	-8.76	-1.1	3.90	SER 293	S 18	H-donor
		-2.2	3.29	SER 293	O 46	H-acceptor
		-0.7	4.15	TYR 337	C 83	H-pi
		-0.6	4.25	TYR 341	C 85	H-pi
6c	-6.93	-3.2	3.01	GLU 202	O 38	H-donor
		-2.5	2.59	GLN 71	O 55	H-donor
		-0.6	3.17	GLY 122	O 44	H-acceptor
		-0.0	3.40	TYR 341	6-ring	pi-pi
6d	-8.41	-1.7	2.73	HIS 447	O 21	H-donor
		-0.9	3.09	ASP 74	C 29	H-donor
Donepezil	-7.74	-0.7	3.63	TYR 337	C 36	H-pi
Rivastigmine	-6.39	-0.6	4.13	TRP 86	C 5	H-pi
Tacrine	-5.77	-0.7	3.75	TYR 341	C 20	H-pi
		-2.7	4.04	TRP 86	N 27	H-pi

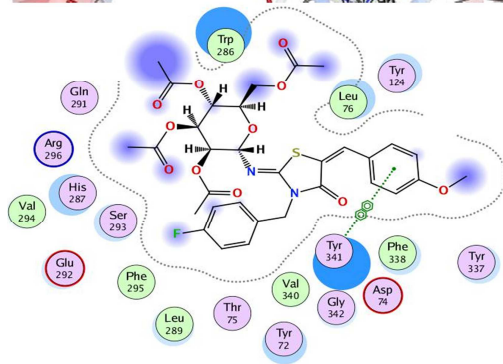
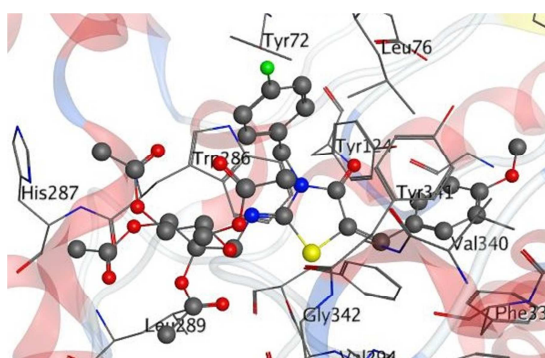


Figure 6: 3D& 2D interaction of **5a** in the active site of AChE (PDB ID: 4EY7)

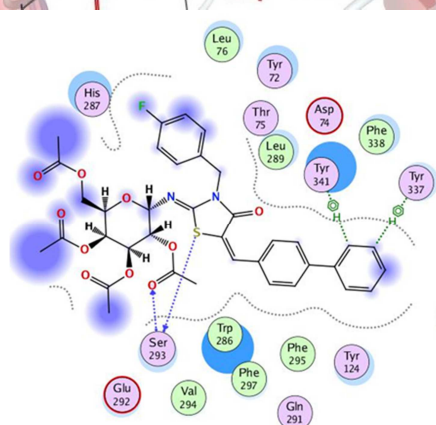
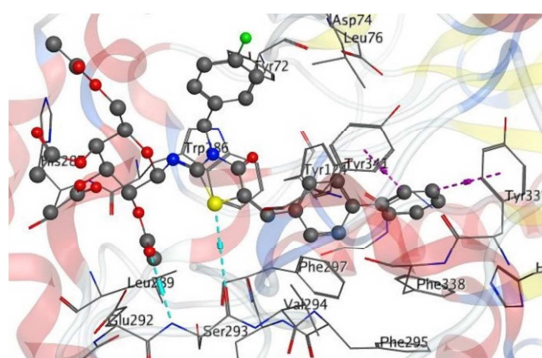


Figure 7: 3D& 2D interaction of **5f** in the active site of AChE (PDB ID: 4EY7). Hydrogen bonds are displayed in cyan & H-pi-bonds in dark magenta

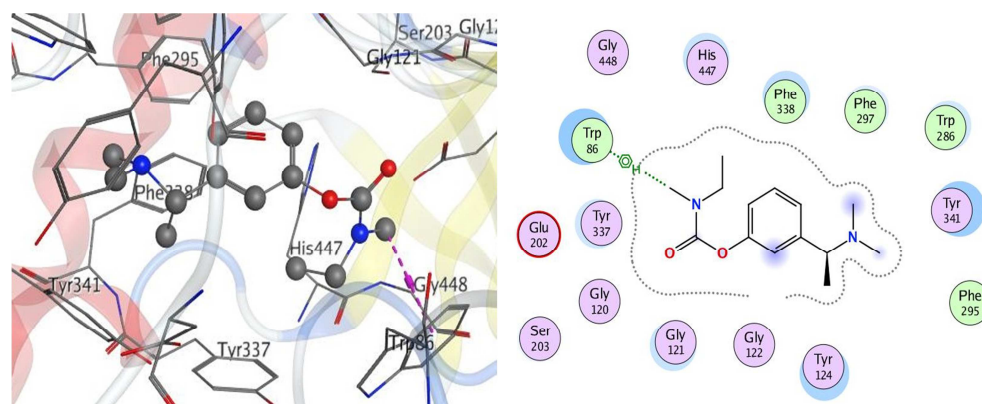


Figure 11: 3D& 2D interaction of **rivastigmine** in the active site of AChE (PDB ID: **4EY7**). H-pi-bonds are displayed in dark magenta

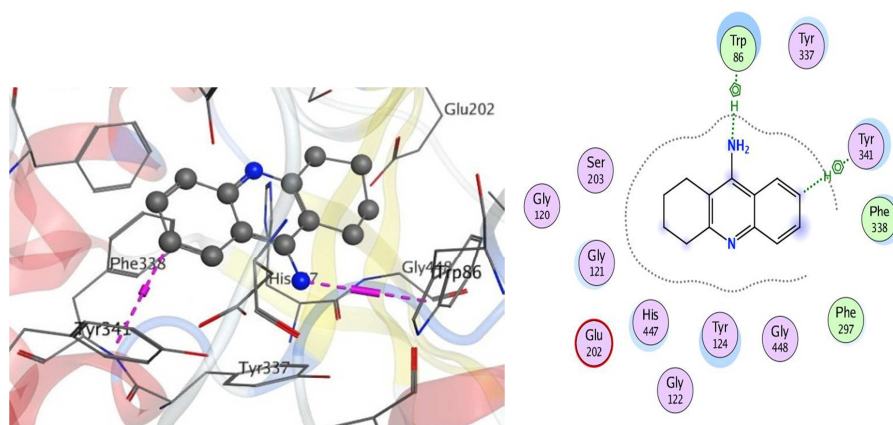


Figure 12: 3D& 2D interaction of **tacrine** in the active site of AChE (PDB ID: **4EY7**). H-pi-bonds are displayed in dark magenta

3.3. In Silico ADMET studies

The ADMET profile of (**5a**, **5f**, **6c** and **6d**) compared to donepezil, rivastigmine and tacrine.

The SwissADME Web tool (www.SwissADME.ch), and the online software PreADMET were used to investigate the pharmacokinetics and toxicity prediction of compounds **5(a,f)**, and **6(c,d)**, as well as the references donepezil, rivastigmine and tacrine. According to the Boiled-egg model [47], and unlike the drug references the compounds **5(a,f)** and **6(c,d)** had low gastrointestinal absorption (GI), therefore, it is believed that P-glycoprotein removes them from the central nervous system. Furthermore, the target compounds showed poor BBB permeability, suggesting they would not be able to enter the central nervous system (CNS) (table 3). Furthermore, compounds **5a**, and rivastigmine were

shown not to bind to P-glycoproteins, in contrast to **5f**, **6(c,d)** the references donepezil, and tacrine.

Moreover, the compounds' interactions with cytochromes P450 (CYP) in the liver, the primary factor for drug removal through metabolic biotransformation, have been studied. Similar to rivastigmine the compounds **5f**, and **6(c,d)** are expected to inhibit none of the cytochrome P-450 (CYP) isoforms in the liver, allowing for the usage with other medications without risk. Compound **5a** is indicated to inhibit just one of the hepatic CYP isoforms (CYP2D6), hence, it should be administered at a separate time than the patient's other medications to avoid potentially dangerous drug interactions. Donepezil and tacrine were discovered to inhibit two of the five major isoforms of hepatic cytochrome P-450 (CYP) (Table 3).

Table 3. The *in silico* predicted pharmacokinetics for compounds **5(a,f)**, **6(c,d)**, donepezil, rivastigmine and tacrine

Molecule	GI absorption	BBB permeant	Pgp substrate	CYP1A2 inhibitor	CYP2C19 inhibitor	CYP2C9 inhibitor	CYP2D6 inhibitor	CYP3A4 inhibitor
5a	Low	No	No	No	No	No	Yes	No
5f	Low	No	Yes	No	No	No	No	No
6c	Low	No	Yes	No	No	No	No	No
6d	Low	No	Yes	No	No	No	No	No
Donepezil	High	Yes	Yes	No	No	No	Yes	Yes
Rivastigmine	High	Yes	No	No	No	No	No	No
Tacrine	High	Yes	Yes	Yes	No	No	No	Yes

3.4. Physicochemical properties, drug-likeness, and toxicity studies.

The most potent compounds, **5(a,f)** and **6(c,d)**, were subjected to a bioinformatics analysis to foretell their physicochemical and drug-like features. Table 4 lists the chemical and physical properties of compounds **5(a,f)**, **6(c,d)**, donepezil, rivastigmine, and tacrine. Because they have molecular weights greater than 500 Da, the target compounds have trouble diffusing and being absorbed across the cell membrane, unlike the drugs used as standards.

The compounds **5(a,f)** and **6(c,d)** have been found to contain Hydrogen bond acceptors (8-13) and Hydrogen bond donors (0-4), allowing some of them to passively penetrate the water-filled gaps of live cell membranes. In addition, both compounds **6c** and **6d** have six rotatable bonds, all of which are attached to a heavy atom, suggesting excellent molecular flexibility. The polar atoms of the

molecule, on the other hand, generated similar mild TPSA to that shown in **6d**. According to the Lipinski rule of five, drugs with an M.wt below 500, an HBD below 5, and an HBA below 10 have satisfactory absorption and bioavailability. There are three of the five criteria that the target compounds follow in terms of their physical and chemical characteristics (Table 4). Regarding toxicity, compounds **6c** and **6d** are not mutagens, however the other examined compounds and referred medications are. Furthermore, compound **5f**, like donepezil and rivastigmine, is not carcinogenic to mouse, but the other compounds studied and tacrine are. In relation to cardiotoxicity (hERG inhibition), compound **5f** has a low risk as a rivastigmine medicine, whereas the other compounds have a medium risk as donepezil and tacrine pharmaceuticals (Table 4).

Table 4. *In silico* physicochemical properties and toxicity predictions for compounds **5(a,f)**, **6(c,d)**, donepezil, rivastigmine and tacrine

Molecule	^a MW ≤ 500	^b HBA ≤ 10	^c HBD ≤ 5	^d TPSA Å ² < 160	^e NRB ≤ 10	^f Log S	#Heavy atoms	Lipinski #violations	Ames_ test	Carcino_ Mouse	Carcino_ Rat	hERG_ inhibition
5a	672.67	13	0	181.63	14	-5.57**	47	2	Mutagen	Positive	Negative	Medium_risk
5f	718.74	12	0	172.4	14	-8.51***	51	2	Mutagen	Negative	Negative	Low_risk
6c	520.53	10	5	177.58	6	-8.51***	36	2	Non-mutagen	Positive	Negative	Medium_risk
6d	517.57	8	4	151.36	6	-8.51***	36	2	Non-mutagen	Positive	Negative	Medium_risk
Donepezil	379.49	4	0	38.77	6	-4.81**	28	0	Mutagen	Negative	Negative	Medium_risk
Rivastigmine	250.34	3	0	32.78	6	-2.69*	18	0	Mutagen	Negative	Negative	Low_risk
Tacrine	198.26	1	1	38.91	0	-3.27*	15	0	Mutagen	Positive	Negative	Medium_risk

^aMW, molecular weight; ^bHBA, number of H-bond acceptors; ^cHBD, number of H-bond donors; ^dTPSA, topological polar surface area; ^eNRB, number of rotatable bonds; ^fLog S, Aqueous solubility (*soluble, **moderately soluble, ***poorly soluble)

3.5. Material and methods

3.5.1. Modeling Drug Action Using Pharmacophores

The following procedures describe how to develop pharmacophores. The five AChE inhibitors shown in figure 1 were used as a training set for the MOE 2015.10 flexible alignment algorithm. The information is available in the result of the flexible alignment (S: Score of configuration alignment). Potentially more successful alignments may be achieved with smaller S values. Copy the S value that is lowest in the alignment structure into the MOE window. For the substances that served as the training set for the alignment, construct a

pharmacophore query in the Pharmacophore Query Editor. Pharmacophore Search is used to check the created model against the whole dataset (**5a,f** and **6c,d**). The software employs a pharmacophore method for labelling the molecular conformations in the test set through the Pharmacophore Preprocessor and its PCH-All (Polarity-Charge-Hydrophobicity) implementation. After that, you can use the consensus query technique to fine-tune the question and go even deeper into the data. Root-mean-square deviation (rmsd) between a given molecule and a hypothetical version generated by the computer are shown in **table 5**.

Table 5. Training inhibitor pharmacophoric and structural characteristics & rmsd values for the hit set

Pharmacophoric features	Structure features	Compound	Rmsd
F1: Hyd/Aro	six heterocycles (pyran ring, benzene ring), -CH ₃ .	5a	0.1562
F2: Hyd/Aro	five heterocycles (thiazolidine ring), six heterocycles (pyran ring, benzene ring), -CH ₂ -O-	5f	0.1006
		6c	0.1277
		6d	0.2375
F3: ML/Acc/Don	C=O, =N-, OH.		

3.6. Results and discussion

3.6. 1. Development of Pharmacophores

The optimal pharmacophore model (hypothesis) was tested by analysing data from a training set consisting of five AChE inhibitors and a test set consisting of four AChE inhibitors [48]. The three stages below outline a typical use of 3D pharmacophores: The first step is to create a three-dimensional model of molecules with known biological activity using a training set. The pharmacophoric qualities come later. Finally, we use a technique for exploring databases for novel compounds with the requisite pharmacophoric properties [49]. How well a chemical map to a created hypothetical model associated to its activity is quantified by the root-mean-squared deviation (rmsd) between the query and its ligand-target sites. H-bond acceptors (Acc), donors (Don), charged/ionizable groups (Cat and Ani), hydrophobic (Hyd), metal ligators (ML), and aromatic rings (Aro) are all examples of classic pharmacophoric features. **Table 5** and figure 13 both provide the tabulated and graphical findings from the first pharmacophoric study.

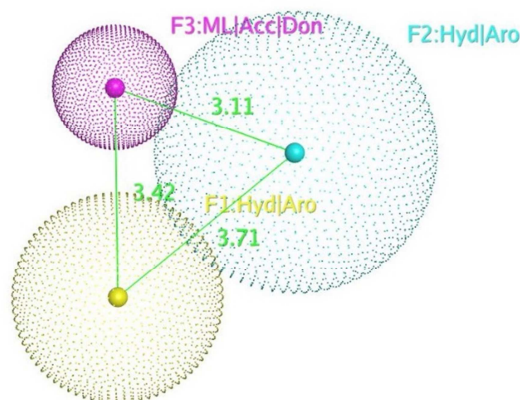


Figure 13: Pharmacophore features and distances

As seen in **table 5**, the rmsd has a greater inhibitory impact as it declines. The maximum activity was seen in superpositions of compound **5f** with rmsd values of 0.1006 (**Fig. 14**). Compounds **5a**, **6c**, and **6d** showed potent inhibitory action as well (rmsd values of 0.1562, 0.1277 and 0.2375, respectively (**Fig. 15-17**)). This suggests that biological testing will provide positive findings.

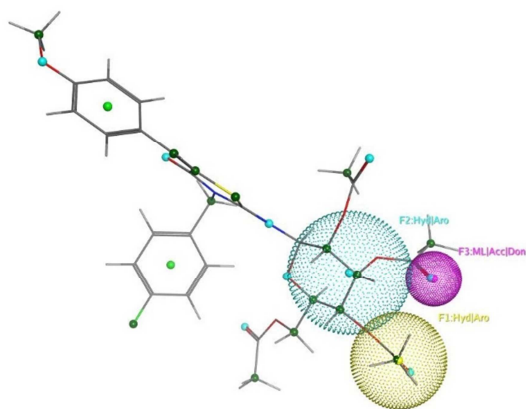


Figure 14: Superposition of **5a** with the query

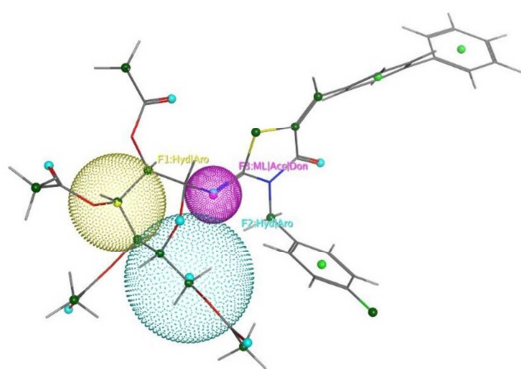


Figure 15: Superposition of **5f** with the query

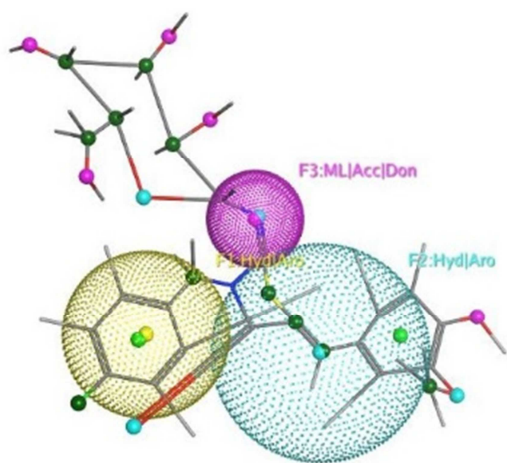


Figure 16: Superposition of **6c** with the query

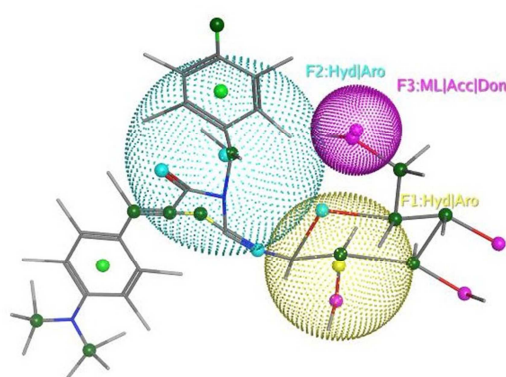


Figure 17: Superposition of **6d** with the query

4. Conclusion

This study focuses on synthesizing thiazolidin-4-one N-glycosides from glucose isothiocyanate and evaluating their inhibitory effects on acetylcholinesterase (AChE), including molecular docking and SAR analyses. Compound **5a** displayed the highest AChE inhibition ($IC_{50} = 0.209 \mu\text{g/mL}$), surpassing rivastigmine and Tacrine, approaching donepezil's potency. The results from the design and biological testing of thiazolidine derivatives were corroborated by *in silico* molecular docking studies. The strong binding affinity and multiplicity of interactions of these compounds with the protein suggest that they will be further developed for application in pharmacological and therapeutic studies. The effectiveness of pharmaceuticals in the clinic depends heavily on their absorption, distribution, and metabolic qualities. Therefore ADMET screening is used to show the ADMET properties of the more potent compounds (**5a,f**, and **6c,d**). The spatial arrangement of the structural components responsible for a certain biological action is known as the pharmacophore. That's why pharmacophore models were constructed using five different AChE inhibitors. We demonstrated the efficacy of synthetic compounds (**5a,f**, and **6c,d**) designed to inhibit AChE by identifying effective and selective inhibitors of this enzyme using 3D pharmacophore virtual screening.

Acknowledgments: The authors extend their appreciation to the deanship of scientific research at Shaqra university for funding this research work. This project was funded by the Deputyship for Research & Innovation, Ministry of Education in Saudi Arabia. Project number (IFP2021-095).

Author Contributions: All authors participated in the experimental work, analysis the data, writing and revised the article

Informed Consent Statement: Not applicable

Data Availability Statement: The data presented in this study are available.

5. References

- [1] World Health, O. Towards a Dementia Plan: A WHO Guide; World Health Organization: Geneva, Switzerland, (2018).
- [2] Prince, M., Knapp, M., Guerchet, M.M., Prina, M.P., Comas-Herrera, A., Wittenberg, R., Adelaja, B., Hu, B., King, D., Rehill, A., et al. Dementia UK: Update, 2nd ed.; © Alzheimer's Society 2014. All rights reserved; Alzheimer's Society: London, UK, ISBN 978-1-906647-31-5(2014).
- [3] Niu, H., Álvarez-Álvarez, I., Guillén-Grima, F., Aguinaga-Ontoso: I. Prevalence and incidence of Alzheimer's disease in Europe: A meta-analysis. *Neurologia*, 32, 523–532(2017).
- [4] Prince, M., Bryce, R., Albanese, E., Wimo, A., Ribeiro, W., Ferri, C.P.: The global prevalence of dementia: A systematic review and metaanalysis. *Alzheimer's Dement. J. Alzheimer's Assoc.* 9, 63–75.e62(2013).
- [5] Spilovska, K., Zemek, F., Korabecny, J., Nepovimova, E., Soukup, O., Windisch, M., Kuca, K.: "Adamantane – A Lead Structure for Drugs in Clinical Practice," *Curr. Med. Chem.* vol. 23, no. 29, pp. 3245–3266(2016).
- [6] Kuca, K., Soukup, O., Maresova, P., Korabecny, J., Nepovimova, E., Klimova, B., Honegr, J., Ramalho, T. C., and T. C. C. Franç: "Current Approaches Against Alzheimer's Disease in Clinical Trials," *J. Braz. Chem. Soc.* Vol. 27, No. 4, 641–649(2016).
- [7] Selkoe, D. J.: "Alzheimer's Disease: Genes, Proteins, and Therapy," *Physiol Rev.* vol. 81, no. 2, pp. 741–766(2001).
- [8] Karran, E., Mercken, M., De Strooper, B.: "The amyloid cascade hypothesis for Alzheimer's disease: an appraisal for the development of therapeutics," *Nat. Rev. Drug Discov.* vol. 10, no. 9, pp. 698–712(2011).
- [9] Francis, P. T., Palmer, A. M., Snape, M., Wilcock, G. K.: "The cholinergic hypothesis of Alzheimer's disease: a review of progress," *J. Neurol Neurosurg Psychiatry* vol. 66, no. 2, pp. 137–147(1999).
- [10] Ballatore, C., Lee, V. M.-Y., Trojanowski J. Q.: "Tau-mediated neurodegeneration in Alzheimer's disease and related disorders," *Nat. Rev. Neurosci.* vol. 8, no. 9, pp. 663–672(2007).
- [11] Webber, K.M., Raina, A. K., Marlatt, M. W., Zhu, X., Prat, M. I., Morelli, L., Casadesus, G., Perry, G., Smith, M. A.: "The cell cycle in Alzheimer disease: A unique target for neuropharmacology," *Mech. Ageing Dev.* vol. 126, no. 10, pp. 1019–1025 (2005).
- [12] Tapia-Arancibia, L., Aliaga, E., Silhol, M., Arancibia, S.: "New insights into brain BDNF function in normal aging and Alzheimer disease," *Brain Res. Rev.* vol. 59, no. 1, pp. 201–220(2008).
- [13] Su, B., Wang, X., Nunomura, A., Moreira, P. I., Lee, H. G., Perry, G., Smith, M. A., Zhu, X.: "Oxidative Stress Signaling in Alzheimers Disease," *Curr. Alzheimer Res.* vol. 5, no. 6, pp. 525–532(2008).
- [14] Barnham, K. J., Masters, C. L., Bush, A. I.: "Neurodegenerative diseases and oxidative stress," *Nat. Rev. Drug Discov.* vol. 3, no. 3, pp. 205–214 (2004).
- [15] Jomova, K., Valko, M.: "Advances in metal-induced oxidative stress and human disease," *Toxicology* vol. 283, no. 2–3, pp. 65–87 (2011)
- [16] Devi, L., Anandatheerthavarada, H. K., "Mitochondrial trafficking of APP and alpha synuclein: Relevance to mitochondrial dysfunction in Alzheimer's and Parkinson's diseases," *Biochimica et Biophysica Acta (BBA) - Molecular Basis of Disease*, vol. 1802, no. 1, pp. 11–19 (2010).
- [17] Sevigny, J.; Chiao, P.; Bussière, T.; Weinreb, P.H.; Williams, L.; Maier, M.; Dunstan, R.; Salloway, S.; Chen, T.; Ling, Y.; et al.: The antibody aducanumab reduces Aβ plaques in Alzheimer's disease. *Nature* 537, 50–56 (2016).
- [18] Birks, J.: Cholinesterase inhibitors for Alzheimer's disease. *Cochrane Database Syst. Rev.* (2006)
- [19] Srour, A.M., Abd El-Karim, S.S., Saleh, D.O., El-Eraky, W.I., Nofal, Z.M.: Rational design, synthesis and 2D-QSAR study of novel vasorelaxant active benzofuran-pyridine hybrids, *Bioorg. Med. Chem. Lett.* 26 2557–2561(2016).
- [20] Vitaku, E., Smith, D.T., Njardarson, J.T.: Analysis of the structural diversity, substitution patterns, and frequency of nitrogen heterocycles among U.S. FDA approved pharmaceuticals. *J. Med. Chem.* 57:10257–74 (2014).
- [21] Bosenbecker, J., Bareno, V.D.O., Difabio, R., et al.: Synthesis and ~ antioxidant activity of 3-(pyridin-2-yl,ethyl)-1,3-thiazinan(thiazolidin)-4-ones. *J. Biochem. Mol. Toxic.* 28:425–32(2014).
- [22] Bielenica, A., Sanna, G., Madeddu, S., et al.: New thiourea and 1,3-thiazolidin-4-one derivatives effective on the HIV-1 virus. *Chem. Biol. Drug Des.* 90:883–91 (2017).

- [23] Ansari, M.F., Idrees, D., Hassan, M.I., et al.: Design, synthesis and biological evaluation of novel pyridine-thiazolidinone derivatives as anticancer agents: targeting human carbonic anhydrase IX. *Eur. J. Med. Chem.* 144:544–56 (2018).
- [24] DaSilva, D.S., DaSilva, C.E.H., Soares, M.S.P., et al.: Thiazolidin-4-ones from 4-(methylthio)benzaldehyde and 4-(methylsulfonyl)benzaldehyde: synthesis, antiangioma activity and cytotoxicity. *Eur. J. Med. Chem.* 124:574–82 (2016).
- [25] Gouvea, D.P., Vasconcelos, F.A., Berwaldt, G.A., et al.: 2-Aryl-3-(2-morpholinoethyl)thiazolidin-4-ones: synthesis, anti-inflammatory in vivo, cytotoxicity in vitro and molecular docking studies. *Eur. J. Med. Chem.* 118:259–65 (2016).
- [26] Patel, N.B., Patel, M.D.: Synthesis and evaluation of antibacterial and antifungal activities of 4-thiazolidinones and 2-azetidiones derivatives from chalcone. *Med. Chem. Res.* 26: 1772–83 (2017).
- [27] Raza, S., Srivastava, S.P., Srivastava, D.S., et al.: Thiazolidin-4-one and thiazinan-4-one derivatives analogous to rosiglitazone as potential antihyperglycemic and antidyslipidemic agents. *Eur. J. Med. Chem.* 63:611–20 (2013).
- [28] Jiao, H.; Jia, J.: Ginsenoside compound K acts via LRP1 to alleviate Amyloid β (42)-induced neuroinflammation in microglia by suppressing NF- κ B. *Biochem. Biophys. Res. Commun.* 590, 14–19 (2022).
- [29] Alshamari, A. K., Elsawalhy, M., Alhajri, A. M., Hassan, A. A., Elharrif, M. G., Sam, G., Alamshany, Z. M., Alshehri, Z. S., Alshehri, F. F., Hassan, N. A.: Design, Synthesis, Molecular Docking and Biological Evaluation of Donepezil Analogues as Effective Anti-Alzheimer Agents, *Egyptian Journal of Chemistry*, Available Online from 27 September 2023. doi: 10.21608/EJCHEM.2023.231046.8475
- [30] Hassan, N. A., Hegab, M. I., Rashad, Aymn. E., Fahmy, A. A., Abdel-Megeid, F. M. E.: "Synthesis And Antimicrobial Activity Of Some Cyclic And Acyclic Nucleosides Of Thieno[2,3-d]Pyrimidines," *Nucleosides Nucleotides Nucleic Acids* vol. 26, no. 4, pp. 379–390 (2007).
- [31] El-Sayed, H.A., Moustafa, A.H., Hassan, A.A., El-Seadawy, N.A.M., Pasha S.H., Shmiess N. A.M., Awad, H.M., Hassan, N.A.: "Microwave synthesis, anti-oxidant and anti-tumor activity of some nucleosides derived 2-oxonicotinonitrile," *Synth. Commun.* vol. 49, no. 24, pp. 3465–3474 (2019).
- [32] Khattab, R. R., Alshamari, A. K., Hassan, A. A., Elganzory, H. H., El-Sayed, W. A., Awad, H. M., Nossier, E.S., Hassan, N.A.: "Click chemistry based synthesis, cytotoxic activity and molecular docking of novel triazole-thienopyrimidine hybrid glycosides targeting EGFR," *J. Enzyme. Inhib. Med. Chem.* vol. 36, no. 1, pp. 504–516 (2021).
- [33] Basiony, E.A., et al.: "Synthesis and Cytotoxic Activity of New Thiazolopyrimidine Sugar Hydrazones and Their Derived Acyclic Nucleoside Analogues," *Molecules* vol. 25, no. 2, p. 399 (2020).
- [34] Tashkandi, N.Y., Al-Amshany, Z.M., Hassan, N.A.: "Design, synthesis, molecular docking and antimicrobial activities of novel triazole-ferulic acid ester hybrid carbohydrates," *J. Mol. Struct.* vol. 1269, p. 133832 (2022).
- [35] Hassan, N. A., Alshamari, A. K., Hassan, A. A., Elharrif, M. G., Alhajri, A. M., Sattam, M., Khattab R.R.: "Advances on Therapeutic Strategies for Alzheimer's Disease: From Medicinal Plant to Nanotechnology," *Molecules* 27(15):4839 (2022).
- [36] Liu, K.; Cui, H.F.; Nie, J.; Dong, K.Y.; Li, X.J.; Ma, J.A. Highly enantioselective michael addition of aromatic ketones to nitroolefins promoted by chiral bifunctional primary amine-thiourea catalysts based on saccharides. *Org. Lett.* 9, 923–925 (2007).
- [37] Gao, P.; Wang, C.G.; Wu, Y.; Zhou, Z.H.; Tang, C.C., *Eur. J. Org. Chem.* 27, 4563–4566 (2008).
- [38] Redemann, C. E.; Niemann, C. Acetobromoglucose. *Org. Synth.* 1942, 22, 1–5.
- [39] Zhang, M., Zhu, W., Li, Y.: Discovery of novel inhibitors of signal transducer and activator of transcription 3 (STAT3) signaling pathway by virtual screening., *European Journal of Medicinal Chemistry*, 62, 301–310 (2013). doi.org/10.1016/j.ejmech.2013.01.009
- [40] Manasa, K., Sandip, P., Geetanjali, D., Joel, G., Regur, P., Arbaz, S. S., Dilep, K. S., Chandraiah, G., Narayana, N., Neelima, D.T., Nagula, S. : "Design, synthesis of DNA-interactive 4-thiazolidinone-based indolo- pyrroloazepinone conjugates as potential cytotoxic and topoisomerase I inhibitors" *European Journal of Medicinal Chemistry* 238 (2022). https://doi.org/10.1016/j.ejmech.2022.114465
- [41] Moghaddam, F. M., Hojabri, L. : "A Novel Synthesis of Some 2-Imino-4-thiazolidinone Derivatives" *J. Heterocyclic Chem.*, 44, 35 (2007).
- [42] Jieun, L., Yu, J. P., Hee, J. J., Sultan, U., Dahye, Y., Yeongmu, J., Ga, Y. K., Min, K.g K., Dongwan, K., Yujin, P., Pusoon, C., Hae, Y. C., Hyung, R. M.:" Design and Synthesis of (Z)-2-(Benzylamino)-5-benzylidenethiazol-4(5H)-one Derivatives as Tyrosinase Inhibitors and Their Anti-Melanogenic and Antioxidant Effects ,

- Molecules*, 28 (2), 848 (2023). <https://doi.org/10.3390/molecules28020848>
- [43] Firouz, M. M., Leila H.: "A Novel Synthesis of Some 2-Imino-4-thiazolidinone Derivatives" *J. Heterocyclic Chem.*, 44, 35 (2007).
- [44] Denis, R. St., Laurent, Q. G., Dedong, Wu., Michael, H. Serrano – Wu.: "Regioselective synthesis of 3-(heteroaryl)-iminothiazolidin-4-ones" *Tetrahedron Letters* 45, 1907–1910 (2004). doi: 10.1016/j.tetlet.2004.01.001
- [45] NGUYEN, D, T.: "Reaction of N-(Per-O-acetyl- β -D-glucopyranosyl)-N'-(4',6'-diarylpyrimidine-2'-yl) thioureas with Ethyl Bromoacetate" *E-Journal of Chemistry* 8 (3), 1355-1361 (2011).
- [46] Full crystallographic data have been deposited to the Cambridge Crystallographic Data Centre (CCDC 265765). Copies of the data can be obtained free of charge via the internet at <http://www.ccdc.cam.ac.uk>
- [47] Diana, A., Zoete, V.A: BOILED-Egg to Predict Gastrointestinal Absorption and Brain Penetration of Small Molecules. *Chem. Med. Chem. II*, 1117–1121(2016).
- [48] Yang, J. M., Shen, T.W., Chen, Y.F., Chiu, Y.Y.: An evolutionary approach with pharmacophore-based scoring functions for virtual database screening. In Genetic and Evolutionary Computation Conference (pp. 481-492). Springer, Berlin, Heidelberg (2004).
- [49] Mason, J., Good, A., Martin, E.: 3-D Pharmacophores in Drug Discovery. *Current Pharmaceutical Design* 7(7), 567–597 (2001).